JOURNAL OF Materials CHEMISTRY

N-Acyl-*β*-D-glycopyranosylamines containing 1,4-disubstituted cyclohexyl and phenyl rings: mesomorphism and molecular structure relationships

David F. Ewing,[a] Mandy Glew,[a] John W. Goodby,[a] Julie A. Haley,[a] Stephen M. Kelly,*[a†‡] Bernd U. Komanschek,[b] Philippe Letellier,[a] Graham Mackenzie*[a] and Georg H. Mehl[a]

[a] *The School of Chemistry, Hull University, Hull, UK HU6 7RX*

[b] *CCLRC Daresbury, Daresbury, UK*

A variety of *N*-acyl-*β*-D-glycopyranosylamines incorporating aliphatic and/or aromatic groups has been prepared regiospecifically and in good yield in a one step reaction of the required acid chloride with commercially available D-glycosylamines. The dependence of mesophase behaviour on the degree and nature of intermolecular hydrogen bonding, as well as the size and nature of the hydrophilic and hydrophobic parts of the core and the linking groups between the two have been studied. Of the compounds investigated only the *N*-(4-alkoxybenzoyl)-*β*-D-glucopyranosylamines and *N*-(*trans*-4-pentylcyclohexylacetyl)-*β*-D-glucopyranosylamine exhibited an observable thermotropic liquid crystal phase. The compounds synthesized were essentially insoluble in water and no lyotropic mesomorphism was observed. It is clear that it is the number of groups on the hydrophilic carbohydrate part of the molecule capable of hydrogen bonding, after a crucial length of the hydrophobic part of the molecule has been attained, that primarily determines thermotropic mesophase behaviour. However, it has also been found that an odd number of units in the central linkage between the hydrophilic and lipophilic parts of the molecule leads to significantly higher transition temperatures than those of compounds incorporating linkages with an even number of units. X-Ray diffraction studies imply that there is no intercalation of the hydrophobic parts of the molecule in the crystalline state. However, some intercalation is thought to occur after melting to form the bilayer structure of the smectic A* phase.

Glycolipids with long aliphatic chains have been reported over the last 150 years to exhibit unusual melting behaviour or double melting points.[1–4] It is now clear that these carbohydrates were in fact liquid crystals exhibiting[5–14] lamellar smectic A* (SmA*),[8,13,14] discotic or cubic[15–17] mesophases. Furthermore, glycolipids often possess amphotropic behaviour,[18] since they exhibit liquid crystalline properties both on melting the pure material to generate a thermotropic mesophase and also in the presence of solvents, *e.g.* with water to produce lyotropic mesophases,[19,20] which are also temperature dependent.

The use of derivatives of naturally occurring monosaccharides as solvents for non-denatured proteins,[21,22] antibacterial and antiviral agents,[23,25] surfactants,[26] artificial blood,[27] drug delivery systems,[28] optically active building blocks for chiral nematic and ferroelectric liquid crystals,[29,30] *etc.* has been reported. Furthermore, the structural and biological function of monosaccharides, oligosaccharides and polysaccharides in the organization and function of cell membranes is becoming of increasing interest.[31,32] It is becoming more apparent that the molecular factors determining the type of thermotropic and lyotropic mesophases observed for liquid crystalline carbohydrate derivatives are the configuration of the hydrophilic (carbohydrate) part of the molecule, the number and length of the hydrophobic substituents, such as alkyl chains characteristic of liquid crystalline carbohydrate derivatives, and the degree and strength of hydrogen bonding with neighbouring molecules. The factors that are important are becoming more apparent from evaluation of the large number of modified monosaccharides and oligosaccharides exhibiting thermotropic and lyotropic liquid crystal properties synthesized recently, especially in the last five years.[33–43]

However, the dependence of mesomorphic behaviour on the nature of the linkage between the hydrophilic and hydrophobic parts of liquid crystalline carbohydrates has been studied to a much lesser extent. Therefore, it was decided to synthesise a limited number of derivatives of readily accessible carbohydrates, incorporating the chemically and thermally stable amide linkage at the anomeric position. This would allow investigation of the effect of introducing an additional site for hydrogen bonding next to the carbohydrate core. Initial studies have shown that this can lead to higher melting and clearing points than is observed for related compounds, such as esters or acetals.[44–46] The amide linkage in carbohydrates is of especial interest since it seems to play an important role in the supramolecular structure of diverse, naturally occurring glycoconjugates.[47,48]

Some X-ray diffraction data are available for several of the limited number of liquid crystalline carbohydrate derivatives reported with an amide linkage, but only for the crystalline state.[49,53] Therefore, it was hoped that X-ray diffraction studies on these new compounds in the crystalline and mesomorphic state would yield information on the molecular structure in both of these states. Two related models for the molecular organisation of the lamellar SmA* phase of liquid crystal carbohydrates have been proposed.[10–14] One model for the bilayer lamellar structure of the smectic A* phase found for many carbohydrate derivatives suggests that the layers are held together by hydrogen bonding of the carbohydrate moieties along the median of the layers. The non-interdigitated aliphatic chains form the peripheral regions of the layers.[10] An alternative model proposes that the aliphatic chains are intercalated in the SmA* phase and located at the centre of the layers, whereas the carbohydrate moieties self-assemble in the outer regions of the bilayers.[11–14] Although X-ray diffraction studies primarily carried out on such liquid crystalline carbohydrate derivatives in the crystalline state indicate that intercalation of the alkyl chains is indeed present,[8,13] it is not necessary for there to be any correlation between the ordering in the crystalline state and in the mesomorphic state.[11–14]

†E-mail: s.m.kelly@chem.hull.ac.uk

‡EPSRC advanced fellow.

A limited number of previous investigations had shown that amphiphilic carbohydrate derivatives incorporating aromatic and aliphatic cores commonly found in non-amphiphilic liquid crystals could also exhibit mesomorphism at elevated temperatures.[41–44] Some substituted phenyl derivatives were found to be more water-soluble than the corresponding carbohydrates with an aliphatic carbon chain in place of the aromatic ring.[41] This has potential ramifications for technological applications based on lyotropic solutions of carbohydrate derivatives in water, such as those involving drug delivery, detergents and surfactants, as many thermotropic liquid crystalline sugar derivatives are only sparingly soluble in water at ambient temperatures. Therefore, it was also decided to extend these studies and synthesize a number of compounds related to the recently reported liquid crystalline, *N*-acyl-*β*-D-glycosylamines,[45,46] incorporating aromatic and aliphatic cores. Combinations of cyclohexyl and phenyl rings with terminal and lateral substituents found in typical nonamphiphilic liquid crystals are incorporated in order to clarify whether or not there is any correlation between the thermotropic mesomorphism of amphiphilic and nonamphiphilic liquid crystals incorporating identical moieties in the molecular core. D-Glucopyranosides and D-mannopyranosides were chosen with the appropriate structural diversity in order to study the relationship between molecular shape, chain length, lateral substituents and degree of aromaticity and liquid crystalline behaviour. Primarily, D-glucose derivatives were prepared in order to allow comparisons with known systems to be made as most thermal data reported in the literature for liquid crystal transition temperatures refer to glucose derivatives.[11,12,36–43] Additionally, mannose, xylose and ribose derivatives were prepared in order to investigate the dependence of the mesophase behaviour of this class of compound on sugar configuration.

Experimental

Techniques

The structures of the intermediate and final products were determined by ^{1}H and ^{13}C NMR spectroscopy (JEOL JNM-GX 270 spectrometer), mass spectrometry (Finnigan-MAT 1020 GC–MS spectrometer) and infrared spectroscopy (Perkin-Elmer 457 grating spectrophotometer). ^{1}H chemical shifts were measured, in [$^2H_6$]DMSO, relative to $(CH_3)_4Si$ and ^{13}C chemical shifts relative to the solvent (δ 39.5). *J* Values are in Hz. The ^{1}H and ^{13}C NMR data clearly showed the pyranose form for the derivatised monosaccharides and also indicated the stereochemistry associated with the anomeric centre. The purity of each compound was determined by thin layer chromatography (TLC), high performance liquid chromatography (HPLC), elemental analysis (C, H, N) and differential scanning calorimetry (DSC). 4 × 8 cm precoated TLC plates, SiO_2 SIL G/UV$_{254}$, layer thickness 0.25 mm (Machery-Nagel, Düren, Germany) were utilized.

Column chromatography was carried out using silica gel 60 (230–400 mesh ASTM). Reaction solvents and liquid reagents were purified by distillation or drying shortly before use. Reactions were carried out under dry N_2 unless water was present as a reagent or a solvent. Mesophase identification and the transition temperatures of the carbohydrates synthesised were determined by optical microscopy using either Olympus BH-2 or a Zeiss Universal polarizing light microscope in conjunction with a Mettler FP 82 microfurnace and FP 80 Central Processor. Homeotropic sample preparations suitable for phase characterisation were prepared by using very clean glass microscope slides (washed with water, acetone, water, concentrated nitric acid, water and dry acetone).

Differential scanning calorimetry was used to determine enthalpies of transition and to confirm the phase transition temperatures determined by optical microscopy. Differential scanning thermograms (scan rate 10 °C min^{-1}) were obtained using a Perkin-Elmer DSC 7 PC system operating on DOS software. The results obtained were standardised with respect to indium (measured onset 156.68 °C, ΔH 28.47 J g^{-1}, literature value 156.60 °C, ΔH 28.45 J g^{-1}), nitrotoluene (measured onset 51.17 °C, ΔH 118.49 J g^{-1}, literature value 51.63 °C, ΔH 122.58 J g^{-1}) and benzil (measured onset 94.42 °C, ΔH 108.52 J g^{-1}, literature value 94.87 °C, ΔH 92.68 J g^{-1}).

Comparison of the transition temperatures determined by optical microscopy and differential scanning calorimetry shows some discrepancies of about 1–3 °C. Discrepancies may be due to two factors: firstly, the two methods use different instruments which are calibrated in different ways, and secondly, and more importantly, the carbohydrates tend to decompose at elevated temperatures at various rates depending on the rate of heating, the time spent at an elevated temperature and the nature of the supporting substrate, *e.g.* the materials decomposed more quickly in aluminium DSC pans than on glass microscope slides.

Synthesis of *N*-acyl-*β*-D-glycopyranosylamines from alicyclic and aromatic carboxylic acids

A direct acylation of commercially available D-glycosylamines using triethylamine as a base and *N*,*N*′-dimethylformamide (DMF) as the solvent yielded the desired *N*-acyl-*β*-D-glycosylamines (**1**–**17**) in good yield and purity. The required acid chlorides were either commercially available or were prepared from the corresponding acids by reaction with thionyl chloride. Good selectivity was achieved without the necessity of using thiadiazole reagents.[45] The reaction was stereospecific in all cases, giving only the *β* anomers. The *N*-(*trans*-4-pentylcyclohexylacetyl)-*β*-D-glucopyranosylamine **23** was prepared in a similar fashion utilising *trans*-4-penylcyclohexylacetyl chloride and D-glucosylamine.

General procedure

PCl_5 (1 equiv.) was added in portions to a mixture of the carboxylic acid (1.0 g, 1 equiv.) in THF–diethyl ether (20 cm^3; 1 : 1; v/v) and the resulting mixture stirred until a clear solution was obtained (*ca.* 3 h). The solvent was removed by evaporation under reduced pressure to yield the crude acid chloride, which was dissolved in DMF (20 cm^3) and the resultant solution added dropwise to a solution of *β*-D-glucopyranosylamine (1 equiv.) and DMF (20 cm^3) at room temperature. The reaction mixture was stirred for 3 h, then the solvent was removed by evaporation under reduced pressure (azeotroped with toluene). The crude product was taken up in *n*-butanol and the resultant solution was washed with water (3 × 20 cm^3). The organic phase was evaporated down and the resultant residue purified by column chromatography on silica gel using chloroform–methanol (5 : 1; v/v) as eluent and then recrystallised from ethanol. The white crystals so obtained were dried *in vacuo* over P_2O_5.

N-(*trans*-4-Pentylcyclohexylcarbonyl)-*β*-D-glucopyranosylamine 1

δ_H (DMSO) 0.86 (m, 5H, alkyl), 1.24 (m, 11H, alkyl), 1.74 (m, 4H, alkyl), 2.08 (t, 2H, *J* 7.5, alkyl), 2.98–3.21 (m, 4H, H-2, H-3, H-4, H-5), 3.40 (m, 1H, $J_{5,6'}$ 5, $J_{6,6'}$ 12, H-6′), 3.61 (dd, 1H, $J_{5,6}$ 6, $J_{6,6'}$ 12, H-6), 4.45 (m, 1H, OH), 4.66 (t, 1H, $J_{1,NH}$ 9, H-1), 4.76, 4.85, 5.00 (3 × d, 3H, 3 × OH), 8.19 (d, 1H, $J_{NH,1}$ NHCO). δ_C (DMSO) 13.95, 22.12, 25.95, 28.81, 29.15, 31.61, 32.08, 36.53, 36.84 (alkyl), 60.92 (C-6), 70.01, 72,42, 77.58, 78.49 (C-2–C-5), 79.46 (C-1), 176.56 (*C*ONH). Elemental analysis for $C_{18}H_{33}NO_6$; Calc.: C, 60.14; H, 9.25; N, 3.90; Found: C, 60.54, H, 9.39, N, 3.83%.

N-(*trans*-4-Pentylcyclohexylcarbonyl)-β-D-mannopyranosylamine 2

δ_H (DMSO) 7.79 (NH, *J* 8.15, 1H, d), 4.99–4.69 (4 × OH, 4H, m), 4.42 (H-1, *J* 1.07, 1H, m), 4.33–3.16 (H-2–H-6′, 6H, m), 2.15 (COCH, 1H, m), 1.71 (CH_2, 2H, m), 1.27–1.04 (aliphatic chain, 13H, m), 0.88 (CH_3, 3H, t). δ_C (DMSO) 174.8 (CO), 78.9 (C-1), 77.3 (C-5), 73.9 (C-3), 70.8 (C-2), 66.7 (C-4), 61.3 (C-6), 43.7–18.5 (aliphatic), 13.9 (CH_3). Elemental analysis for $C_{18}H_{33}NO_6$; Calc.: C, 60.14; H, 9.25; N, 3.90; Found: C, 59.98; H, 9.17; N, 3.83%. $[\alpha]_D^{23}$ −1.6 (*c* 0.0146 g cm^{-3}; DMSO); R_f 0.46 chloroform–methanol (2:1).

N-(*trans*-4-Pentylcyclohexylcarbonyl)-β-D-xylopyranosylamine 3

δ_H (DMSO) 8.17 (NH, *J* 8.45, 1H, d), 5.00–4.82 (3 × OH, 3H, m), 4.58 (H-1, *J* 8.31, 1H, m), 3.61–2.99 (H-2–H-5′, 5H, m), 2.05 (COCH, 1H, m), 1.71 (CH_2, 4H, m), 1.30–1.12 (aliphatic, 13H, m), 0.87 (CH_3, 3H, t). δ_C (DMSO) 174.1 (CO), 78.6 (C-1), 76.0 (C-3), 70.5 (C-2), 68.1 (C-4), 65.7 (C-5), 42.5–18.5 (aliphatic), 12.3 (CH_3). Elemental analysis for $C_{17}H_{31}NO_5$; Calc.: C, 61.98; H, 9.49; N, 4.25; Found: C, 61.84; H, 9.21; N, 4.03% $[\alpha]_D^{25}$ +16.6 (*c* 0.0151 g cm^{-3}; DMSO); R_f 0.40 chloroform–methanol (2:1).

N-(4-Pentyloxybenzoyl)-β-D-glucopyranosylamine 4

δ_H (DMSO) 8.74 (NH, *J* 9.45, 1H, d), 7.84, 7.28 (aromatic, J_{ortho} 8.10, 4H, m), 5.03–4.91 (3 × OH, 3H, m), 4.89 (H-1, *J* 8.13, 1H, m), 4.51 (OH, 1H, t), 3.68–3.10 (H-2–H-6′, 6H, m), 1.57 (CH_2, 2H, m), 1.28 (aliphatic, 4H, m), 0.87 (CH_3, 3H, t). δ_C (DMSO) 166.5 (CO), 161.2–114.2 (aromatic), 80.2 (C-1), 78.5 (C-5), 77.6 (C-3), 72.0 (C-2), 70.0 (C-4), 67.2 (OCH_2), 61.0 (C-6), 34.9, 21.9 (aliphatic), 13.9 (CH_3). Elemental analysis for $C_{18}H_{27}NO_7$; Calc.: C, 58.52; H, 7.37; N, 3.79; Found: C, 58.47; H, 7.31; N, 3.77%. $[\alpha]_D^{22}$ +17.2 (*c* 0.0153 g cm^{-3}; DMSO); R_f 0.15 chloroform–methanol (5:1).

N-(4-Hexyloxybenzoyl)-β-D-glucopyranosylamine 5

δ_H (DMSO) 0.86 (m, 3H, alkyl), 1.15–1.40 (m, 6H, alkyl), 1.70 (m, 2H, alkyl), 3.07–3.38 (m, 4H, H-2, H-3, H-4, H-5), 3.43 (m, 1H, $J_{5,6'}$ 5, $J_{6,6'}$ 12, H-6′), 3.67 (dd, 1H, $J_{5,6}$ 6, $J_{6,6'}$ 12, H-6), 4.00 (t, *J* 6.5, OCH_2Ph), 4.50 (t, *J* 6, 1H, OH), 4.87, 4.91 (d, 2H, 2 OH), 4.94 (t, 1H, $J_{1,NH} = J_{1,2}$ 9, H-1), 5.01 (d, 1H, OH), 7.00 and 7.90 (2d, *J* 8, Ph), 8.65 (d, 1H, $J_{NH,1}$ 9, NHCO). δ_C (DMSO) 13.93, 22.09, 25.18, 28.59, 31.19, 61.03 (C-6), 67.68 (alkyl), 70.10, 72.08, 77.63, 78.65 (C-2–C-5), 80.29 (C-1), 113.80, 126.13, 129.52, 161.24, (aromatic), 166.07 (*C*ONH). Elemental analysis for $C_{19}H_{29}NO_7$; Calc.: C, 59.52; H, 7.62; N, 3.65; Found: C, 59.14; H, 7.76; N, 3.59%.

N-(4-Heptyloxybenzoyl)-β-D-glucopyranosylamine 6

δ_H (DMSO) 0.86 (m, 3H, alkyl), 1.15–1.40 (m, 8H, alkyl), 1.70 (m, 2H, alkyl), 3.07–3.38 (m, 4H, H-2, H-3, H-4, H-5), 3.43 (m, 1H, $J_{5,6'}$ 5, $J_{6,6'}$ 12, H-6′), 3.67 (dd, 1H, $J_{5,6}$ 6, $J_{6,6'}$ 12, H-6), 4.02 (t, *J* 6.5, OCH_2Ph), 4.51 (t, *J* 6, 1H, OH), 4.90 (m, 4H, 3 OH, H-1), 6.95 and 7.87 (2d, *J* 8, Ph), 8.65 (d, 1H, $J_{NH,1}$ 9, NHCO). δ_C (DMSO) 13.95, 22.05, 25.45, 28.43, 28.61, 31.31, 61.03 (C-6), 67.64 (alkyl), 70.08, 72.06, 77.63, 78.67 (C-2–C-5), 80.27 (C-1), 113.78, 126.11, 129.51, 161.22 (aromatic), 166.04 (*C*ONH). Elemental analysis for $C_{20}H_{31}NO_7$; Calc.: C, 60.44; H, 7.86; N, 3.52; Found: C, 60.50; H, 7.97; N, 3.41%.

N-(4-Octyloxybenzoyl)-β-D-glucopyranosylamine 7

δ_H (DMSO) 8.66 (NH, *J* 8.64, 1H, d), 7.88–6.98 (aromatic, J_{ortho} 9.45, 4H, m), 5.01–4.90 (3 × OH, 3H, m), 4.90 (H-1, *J* 8.03, 1H, m), 4.56 (OH, 1H, t), 4.02 (OCH_2, 2H, t), 3.65–3.15 (H-2–H-6′, 6H, m), 1.57 (CH_2, 2H, m), 1.35 (aliphatic, 10H, m), 0.88 (CH_3, 3H, t). δ_C (DMSO) 165.9 (CO), 161.1–113.6 (aromatic), 80.2 (C-1), 78.6 (C-5), 77.6 (C-3), 72.0 (C-2), 70.0 (C-4), 67.6 (OCH_2), 61.0 (C-6), 31.2–22.1 (aliphatic), 19.9 (CH_3). Elemental analysis for $C_{21}H_{33}NO_7$; Calc.: C, 61.30; H, 8.08; N, 3.40; Found: C, 61.01; H, 7.91; N, 3.29%. $[\alpha]_D^{22}$ +15.1 (*c* 0.0182 g cm^{-3}; DMSO); R_f 0.13 chloroform–methanol (5:1).

N-(4-Nonyloxybenzoyl)-β-D-glucopyranosylamine 8

δ_H (DMSO) 8.66 (NH, *J* 9.98, 1H, d), 7.89–6.97 (aromatic, J_{ortho} 8.10, 4H, m), 5.11–4.90 (3 × OH, 3H, m), 4.89 (H-1, *J* 8.16, 1H, m), 4.51 (OH, 1H, t), 4.02 (OCH_2, 2H, t), 3.67–3.10 (H-2–H-6′, 6H, m), 1.54 (CH_2, 2H, m), 1.35 (aliphatic, 12H, m), 0.88 (CH_3, 3H, t). δ_C (DMSO) 166.0 (CO), 161–126.1 (aromatic), 80.3 (C-1), 78.7 (C-5), 77.6 (C-3), 72.0 (C-2), 70.0 (C-4), 67.6 (OCH_2), 61.0 (C-6), 31.3–22.1 (aliphatic), 13.9 (CH_3). Elemental analysis for $C_{22}H_{35}NO_7$; Calc.: C, 62.10; H, 8.29; N, 3.29; Found: C, 61.94; H, 8.07; N, 3.19%. $[\alpha]_D^{22}$ +13.9 (*c* 0.0146 g cm^{-3}; DMSO); R_f 0.15 chloroform–methanol (5:1).

N-(4-Decycloxybenzoyl)-β-D-glucopyranosylamine 9

δ_H (DMSO) 8.66 (NH, *J* 8.64, 1H, d), 7.88–6.98 (aromatic, J_{ortho} 9.45, 4H, m), 5.01–4.90 (3 × OH, 3H, m), 4.90 (H-1, *J* 8.03, 1H, m), 4.56 (OH, 1H, t), 4.02 (OCH_2, 2H, t), 3.65–3.15 (H-2–H-6′, 6H, m), 1.57 (CH_2, 2H, m), 1.35 (aliphatic chain, 10H, m), 0.88 (CH_3, 3H, t). δ_C (DMSO) 165.9 (CO), 161.10–113.6 (aromatic), 80.2 (C-1), 78.6 (C-5), 77.6 (C-3), 72.0 (C-2), 70.0 (C-4), 67.6 (OCH_2), 61.0 (C-6), 31.2–22.1 (aliphatic), 13.9 (CH_3). Elemental analysis for $C_{23}H_{37}NO_7$; Calc.: C, 62.85; H, 8.48; N, 3.19; Found: C, 62.82; H, 8.60; N, 3.10%.

N-[4-(*trans*-4-Pentylcyclohexyl)benzoyl]-β-D-glucopyranosylamine 10

δ_H (DMSO) 8.72 (NH, *J* 8.38, 1H, d), 7.82–7.31 (aromatic, J_{ortho} 8.10, 4H, m), 5.01–4.90 (3 × OH, 3H, m), 4.89 (H-1, *J* 7.96, 1H, m), 4.50 (OH, 1H, t), 3.67–3.11 (H-2–H6′, 6H, m), 3.05 (ArCH, 1H, m), 1.81 (CH_2, 4H, m), 1.57–1.05 (aliphatic, 13H, m), 0.88 (CH_3, 3H, t). δ_C (DMSO) 166.5 (CO), 150.9–126.4 (aromatic), 80.2 (C-1), 78.7 (C-5), 77.6 (C-3), 72.1 (C-1), 70.0 (C-4), 61.0 (C-6), 43.7–22.1 (aliphatic), 13.9 (CH_3). Elemental analysis for $C_{24}H_{37}NO_6$; Calc.: C, 66.18; H, 8.56; N, 3.22; Found: C, 66.07; H, 8.31; N, 3.16%. $[\alpha]_D^{22}$ +16.1 (*c* 0.0201 g cm^{-3}; DMSO); R_f 0.12 chloroform–methanol (5:1).

N-[4-(*trans*-4-Pentylcyclohexyl)benzoyl]-β-D-mannopyranosylamine 11

δ_H (DMSO) 8.06 (NH, *J* 8.15, 1H, d), 7.78–7.32 (aromatic, J_{ortho} 8.19, 4H, m), 5.23–4.75 (4 × OH, 4H, m), 4.46 (H-1, *J* 1.10, 1H, t), 3.70–3.16 (H-2–H-6′, 6H, m), 2.75 (ArCH, 1H, m), 1.78 (CH_2, 4H, m), 1.51–1.04 (aliphatic, 13H, m), 0.88 (CH_3, 3H, t). δ_C (DMSO) 165.4 (CO), 151.3–126.7 (aromatic), 79.2 (C-1), 78.0 (C-5), 73.9 (C-3), 70.7 (C-2), 66.8 (C-4), 61.3 (C-6), 43.7–22.1 (aliphatic), 13.9 (CH_3). Elemental analysis for $C_{24}H_{37}NO_6$; Calc.: C, 66.18; H, 8.56; N, 3.22; Found: C, 66.29; H, 8.27; N, 3.18%. $[\alpha]_D^{24}$ −1.4 (*c* 0.0173 g cm^{-3}; DMSO); R_f 0.16 chloroform–methanol (5:1).

N-[4-(*trans*-4-Pentylcyclohexyl)benzoyl]-β-D-xylopyranosylamine 12

δ_H (DMSO) 8.71 (NH, *J* 8.64, 1H, d), 7.81–7.31 (aromatic, J_{ortho} 8.10, 4H, m), 5.06–4.95 (3 × OH, 3H, m), 4.83 (H-1, *J* 9.16, 1H, t), 3.69–3.14 (H-2–H-5′, 5H, m), 3.05 (ArCH, 1H, m), 1.80 (CH_2, 4H, m), 1.47–1.05 (aliphatic, 13H, m), 0.87 (CH_3, 3H, t). δ_C (DMSO) 166.7 (CO), 151.0–126.5 (aromatic), 81.0 (C-1), 77.6 (C-3), 71.9 (C-2), 69.6 (C-4), 67.5 (C-5), 43.7–22.1 (aliphatic), 13.9 (CH_3). Elemental analysis for $C_{23}H_{35}NO_5$; Calc.:

C, 68.12; H, 8.70; N, 3.45; Found: C, 68.07; H, 8.67; N, 3.39%. $[\alpha]_D^{21}$ +5.9 (*c* 0.0159 g cm^{-1}; DMSO); R_f 0.14 chloroform–methanol (5:1).

N-[4-(*trans*-4-Pentylcyclohexyl)benzoyl]-*β*-D-ribopyranosylamine 13

δ_H (DMSO) 8.60 (NH, *J* 8.45, 1H, d), 7.80–7.30 (aromatic, J_{ortho} 8.42, 4H, m), 5.15 (H-1, *J* 9.25, 1H, m), 4.81–4.64 (3 × OH, 3H, m), 3.92–3.42 (H-2–H-5′, 5H, m), 2.50 (ArCH, 1H, m), 1.82 (CH_2, 4H, m), 1.46–1.1 (aliphatic, 13H, m), 0.87 (CH_3, 3H, t). δ_C (DMSO) 166.8 (CO), 150.9–126.5 (aromatic), 76.9 (C-1), 70.9 (C-2), 69.1 (C-3), 67.2 (C-4), 64.2 (C-5), 43.7–22.1 (aliphatic), 13.9 (CH_3). Elemental analysis for $C_{23}H_{35}NO_5$; Calc.: C, 68.12; H, 8.70; N, 3.45; Found: 67.99; H, 8.51; N, 3.43%. $[\alpha]_D^{23}$ −2.6 (*c* 0.0093 g cm^{-3}; DMSO); R_f 0.17 chloroform–methanol (5:1).

N-(4′-(Nonyloxybiphenyl-4-ylcarbonyl)-*β*-D-mannopyranosylamine 14

δ_H (DMSO) 8.21 (NH, *J* 10.8, 1H, d), 7.93–7.03 (aromatic, 4H, m), 5.28–4.73 (4 × OH, 4H, m), 4.48 (H-1, *J* 1.14, 1H, m), 4.02 (OCH_2, 2H, t), 3.72–3.15 (H-2–H-6′, 6H, m), 1.73 (CH_2, 2H, m), 1.30–1.22 (aliphatic, 12H, m), 0.88 (CH_3, 3H, t). δ_C (DMSO) 165.2 (CO), 158.9–114.9 (aromatic), 79.4 (C-1), 78.4 (C-5), 78.1 (C-3), 73.9 (C-2), 70.0 (C-4), 67.5 (OCH_2), 61.2 (C-6), 31.2–22.1 (aliphatic), 13.9 (CH_3). Elemental analysis for $C_{28}H_{39}NO_7$; Calc.: C, 67.04; H, 7.84; N, 2.79; Found: C, 66.91; H, 7.61; N, 2.71%. $[\alpha]_D^{23}$ −2.8 (*c* 0.0100 g cm^{-3}; DMSO); R_f 0.23 chloroform–methanol (5:1).

N-(2′-Fluoro-4′-octyloxybiphenyl-4-ylcarbonyl)-*β*-D-mannopyranosylamine 15

δ_H (DMSO) 8.05 (NH, 1H, t), 7.91–7.02 (aromatic, 7H, m), 5.28–4.77 (4 × OH, 4H, m), 4.47 (H-1, *J* 1.16, 1H, t), 4.01 (OCH_2, 2H, t), 3.69–3.15 (H-2–H-6′, 6H, m), 1.72 (CH_2, 2H, m), 1.41–1.5 (aliphatic, 10H, m), 0.87 (CH_3, 3H, t). δ_C (DMSO) 162.9 (CO), 159.4–114.9 (aromatic), 79.4 (C-1), 77.4 (C-5), 74.5 (C-3), 73.9 (C-2), 70.6 (C-4), 67.6 (OCH_2), 61.2 (C-6), 31.20–22.1 (aliphatic), 13.9 (CH_3). Elemental analysis for $C_{27}H_{36}NO_7F$; Calc.: C, 64.14; H, 7.18; N, 2.77; Found: C, 64.03; H, 7.09; N, 2.73%. $[\alpha]_D^{22}$ −3.9 (*c* 0.0123 g cm^{-3}; DMSO); R_f 0.18 chloroform–methanol (5:1).

N-(2-Fluoro-4′-tetradecyloxybiphenyl-4-ylcarbonyl)-*β*-D-mannopyranosylamine 16

δ_H (DMSO) 8.05 (NH, *J* 8.19, 1H, d), 7.92–7.03 (aromatic, 7H, m), 5.28–4.78 (4 × OH, 4H, m), 4.49 (H-1, *J* 1.10, 1H, t), 4.01 (OCH_2, 2H, t), 3.70–3.16 (H-2–H-6′, 6H, m), 1.72 (CH_2, 2H, m), 1.30–1.24 (aliphatic, 22H, m), 0.87 (CH_3, 3H, t). δ_C (DMSO) 162.0 (CO), 150.3–114.9 (aromatic), 79.4 (C-1), 77.2 (C-5), 74.6 (C-3), 73.0 (C-2), 70.1 (C-4), 67.5 (OCH_2), 61.9 (C-6), 31.2–22.2 (aliphatic), 13.9 (CH_3). Elemental analysis for $C_{33}H_{48}NO_7F$; Calc.: C, 67.21; H, 8.20; N, 2.38; Found: C, 67.12; H, 8.14; N, 2.36%.

N-(2′,3′-Difluoro-4′-octyloxybiphenyl-4-ylcarbonyl)-*β*-D-mannopyranosylamine 17

δ_H (DMSO) 8.25 (NH, 1H, d), 7.52–7.05 (aromatic, 6H, m), 5.24–4.82 (4 × OH, 4H, m), 4.50 (H-1, *J* 1.03, 1H, m), 4.02 (OCH_2, 2H, t), 3.70–3.15 (H-2–H-6′, 6H, m), 1.55 (CH_2, 2H, m), 1.40–1.37 (aliphatic, 10H, m), 0.88 (CH_3, 3H, t). δ_C (DMSO) 162.3 (CO), 155.8–116.4 (aromatic), 85.8 (C-1), 84.6 (C-5), 73.5 (C-3), 72.1 (C-2), 68.2 (C-4), 64.8 (OCH_2), 61.9 (C-6), 32.9–22.9 (aliphatic), 14.4 (CH_3). Elemental analysis for $C_{27}H_{35}NO_7F_2$; Calc.: C, 61.94; H, 6.74; N, 2.68; Found: C, 61.77; H, 6.59; N, 2.54%. $[\alpha]_D^{23}$ −2.5 (*c* 0.0188 g cm^{-3}; DMSO); R_f 0.22 chloroform–methanol (5:1).

Results

Phase characterisation by thermal optical microscopy

All the thermotropic mesophases were found to be of the same type and exhibit the same optical appearance during optical microscopy. For the carbohydrates with an enantiotropic mesophase, the crystals melt on heating at a discrete temperature (T_m) to form a birefringent, fluid texture with an oily streak appearance of webbed focal-conic like defects typical of a SnA* phase, see Fig. 1. Upon further heating the material became optically extinct at the clearing point ($T_{SmA^*\text{-}I}$). Bâtonnets are observed on cooling from this isotropic liquid, which coalesce quickly in the bulk to form focal-conic domains. As each sample was cooled further, the hydrophilic end of the carbohydrate molecules adhered more strongly to the glass surface *via* hydrogen bonding. Thus, most of the resultant textures became homeotropic and optically extinct. These observations indicate that the phase is optically uniaxial (if the mesophase were biaxial then a residual birefringence for the sample would be observed). However, focal-conic defects could still be observed around air bubbles and at the edges of the sample. This optical behaviour, *i.e.* simultaneous presence of both homeotropic and focal-conic textures, indicates that the mesophase is a calamitic smectic A* phase.[8,13,14,33] The notation smectic A* is used to describe the smectic A phase exhibited by these compounds as they are optically active and, therefore, the A* phases formed by them must have reduced symmetry.[33] The characterisation of these defects classifies the mesophase as being smectic A* with a layered structure where the long axes of the molecules are on average orthogonal to the layer planes and the in-plane and out-of-plane positional ordering of the molecules is short range, see X-ray studies.

Differential scanning calorimetry

The enthalpy values for the remaining (T_m) and clearing points ($T_{SmA^*\text{-}I}$) of the *N*-(4-alkoxybenzoyl)-*β*-D-glucopyranosylamines (**4**–**9**) are typical of liquid crystalline carbohydrates (*e.g.* 17.1 and 1.34 J g^{-1}, respectively, for compound **9**). The clearing point enthalpies are relatively small in comparison to the melting enthalpies, and the values measured are of a similar magnitude to those found in conventional liquid crystal systems which exhibit SmA* to isotropic liquid transitions. A typical heating thermogram for the *N*-4-decyloxybenzoyl-*β*-D-glucopyranosylamines **9** is shown in Fig. 2. It is clear that the transitions T_m and $T_{SmA^*\text{-}I}$ are both first-order transitions. The decomposition generally observed at $T_{SmA^*\text{-}I}$ is shown especially clearly in Fig. 2. $T_{SmA^*\text{-}I}$ is often lower on cooling due to

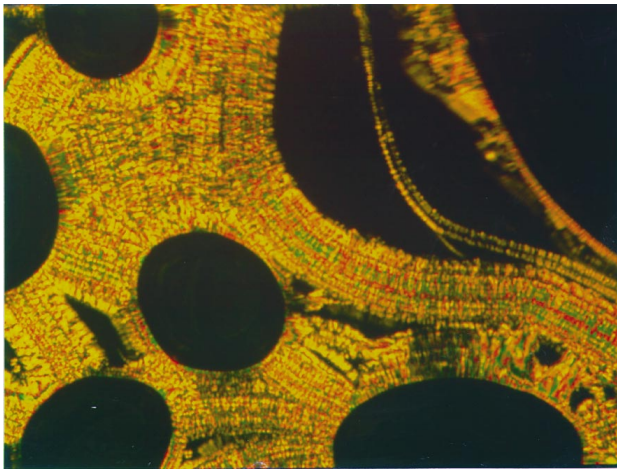

Fig. 1 Photomicrograph at 185 °C of the oily smectic A* texture observed on melting *N*-(4-decyloxybenzoyl)-*β*-D-glucopyranosylamine **9** (magnification × 160)

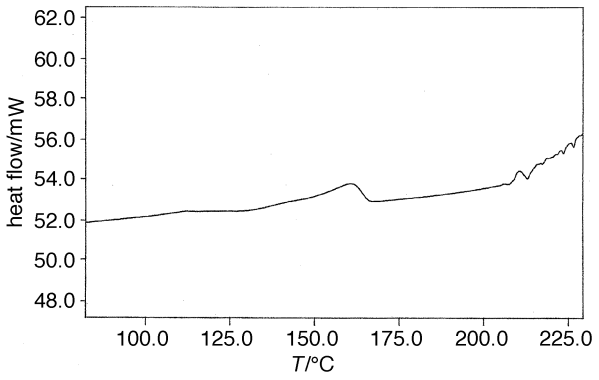

Fig. 2 Differential scanning thermogram as a function of temperature for the first heating cycle for *N*-(4-decyloxybenzoyl)-*β*-D-glucopyranosylamine **9** (scan rate 10 °C min^{-1})

decomposition. On cooling there is a greater tendency to form glasses rather than to recrystallise. The DSC thermogram shown in Fig. 3 for the *N*-(*trans*-4-pentylcyclohexyl-acetyl)-*β*-D-glucopyranosylamine **23** shows T_m and $T_{SmA^*\text{-}I}$ close together followed by thermal decomposition. The thermograms depicted in Fig. 2 and 3 are those observed for the first heating cycle. Thermal decomposition above $T_{SmA^*\text{-}I}$ and the formation of glasses on cooling often led to non-reproducible thermograms for the second or third heating cycles.

Lyotropic mesomorphism

Attempts to obtain lyotropic phases for the new carbohydrate derivatives under the conditions described in the Experimental were unsuccessful as they were all essentially insoluble in water. The presence of one, two or combinations of cyclohexyl and phenyl rings with various chains and lateral substituents in the glycopyranosylamines **1**–**17** does not increase the water solubility of these carbohydrates compared to that of the corresponding *N*-acyl-*β*-D-glycopyranosylamines.[45,46] This is not purely a question of the high T_m of the glycopyranosylamines **1**–**17** as the *N*-(4-alkoxybenzoyl)-*β*-D-glucopyranosylamines **4**–**9** exhibit similar T_m to those of the acyl substituted compounds.[45,46]

X-Ray investigations

In order to characterize the solid state of these materials the aromatic *N*-(4-decyloxybenzoyl)-*β*-D-glucopyranosylamine **9** and the related, but non-aromatic, *N*-octadecanoyl-*β*-D-glucopyranosylamine **28**[45,46] and *N*-octadecanoyl-2-amino-2-deoxy-*β*-D-glucopyranose **29**[45,46] were investigated using X-ray diffraction. The tendency of carbohydrates to decompose at high temperatures required an experimental set-up allowing

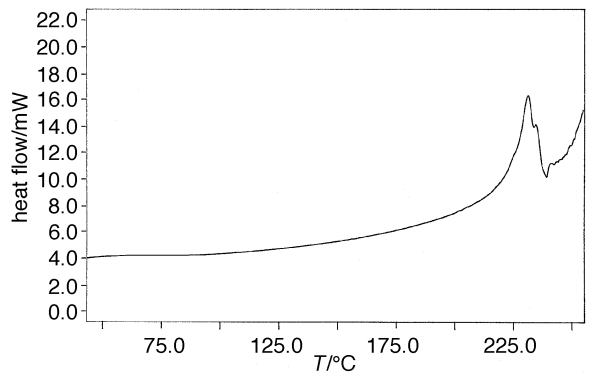

Fig. 3 Differential scanning thermogram as a function of temperature for the first heating cycle for *N*-(*trans*-4-pentylcyclohexylacetyl)-*β*-D-glucopyranosylamine **23** (scan rate 10 °C min^{-1})

for the recording of sufficient data before degradation of the sample sets in. Thus synchrotron radiation was employed, using the experimental set-up of station 8.2 at CCLRC Daresbury, described elsewhere.[54–56]

The samples were prepared as polycrystalline powders in Lindemann tubes and kept at a controlled temperature allowing for the recording of diffraction data whilst performing a temperature scan of 2 °C min^{-1} in the temperature interval of 150 to 210 °C or keeping the sample at a chosen temperatures. The selected experimental set-up was limited to the recording of data relating to lattice parameters greater than 17.8 Å and the use of wet rat-tail collagen as calibration standard led to a systematic error of 3% of the observed *d* spacings.[57]

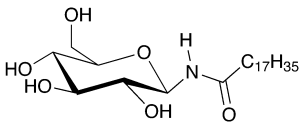

N-octadecanoyl-β-D-glucopyranosylamine **28**: Cr–SmA*, 170 °C; SmA*–I, 220 °C[45,46]

The experimental results for *N*-octadecanoyl-*β*-D-glucopyranosylamine **28**[45,46] are shown in Fig. 4. Throughout the crystalline state reflections relating to lattice parameters of d_1 46.6 Å and d_2 37.2 Å were observable. Whereas the ratio of the intensities of $d_1 : d_2$ is approximately 35 : 1 at 150 °C, a ratio which remains almost constant up to 166 °C, the relative intensity of the reflections relating to d_2 increases sharply above 170 °C with rising temperature. Above that temperature an intensity maximum relating to a *d* spacing d_2 of 37.2 Å could be detected, relating to the full formation of the SmA* phase. The recorded transition temperature of 170 to 172 °C with a biphasic area up to 178 °C is in line with results observed by optical polarizing microscopy and by DSC measurements. Upon reaching the liquid-crystalline state the diffraction pattern coalesced into a meridional maximum, indicative of some macroscopic alignment of the material *via* interactions with the walls of the capillary. Elevation of the temperature led to a reduction in the maximum, in line with a loss of macroscopic ordering. Up to 208 °C the *d* spacing fluctuated between 37.2–35.3 Å. Above that temperature the

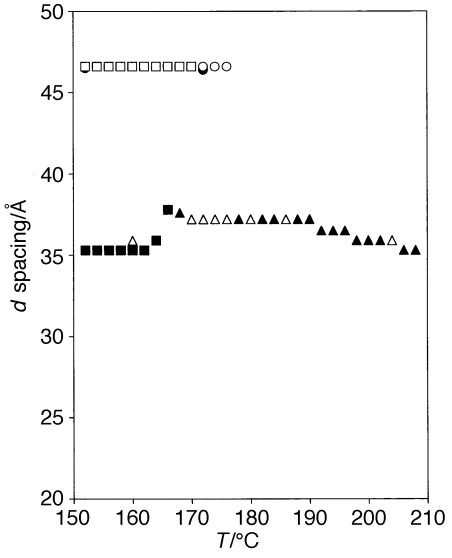

Fig. 4 Variation of the *d* spacings (layer thickness) of *N*-octadecanoyl-*β*-D-glucopyranosylamine **28** with temperature; (□) strong and (■) weak diffraction reflections obtained for the crystalline phase *via* temperature scans at 2 °C min^{-1}, (○) strong and (●) weak reflections for the biphasic region, and (△) strong and (▲) weak reflections for the liquid crystalline region, observed after heating from ambient temperature

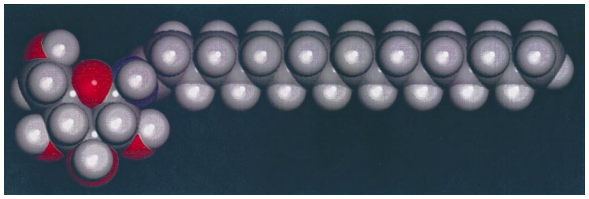

Fig. 5 A model of *N*-octadecanoyl-*β*-D-glucopyranosylamine **28** obtained from CERIUS 2.0

material either reached its liquid state or rapid thermal degradation set in, leading to the absence of small angle intensity maxima. The data recorded by performing a temperature scan of 2 °C min^{-1} are in line with those found by heating samples from ambient temperature and starting the collection of data after thermal equilibrium was indicated by the temperature control unit. The spacing of 46.6 Å at 150 °C indicates that, compared to the overall length of one molecule 26.4 Å [obtained *via* molecular modelling of one molecule in the gas phase at 0 K using the CERIUS 2.0 (MSI) software, see Fig. 5], a bilayer structure must be present in the crystalline state.

The observed values of d_2 of 37.2–35.3 Å in the liquid crystalline state up to the disappearance of the maximum indicate a contraction of the layering with respect to the crystalline modification in the type of an intercalated bipolar structure of the SmA* phase depicted schematically in Fig. 6 and observed earlier for the crystalline phases of diverse liquid-crystalline carbohydrates.[11–14,38,41,52,53,58]

For *N*-4-decyloxybenzoyl-*β*-D-glucopyranosylamine **9**, whose molecular length was determined by molecular modelling, as above, to be 23.4 Å, see Fig. 7, a fundamentally similar temperature dependent phase behaviour was observed. Whereas at 170 °C the material was found to be predominantly crystalline with a lattice parameter d_1 of 41.8 Å, a temperature scan from 180 to 220 °C showed at 180 °C reflections relating to *d* spacings d_1 and d_2 of 41.8 and 37.2 Å and from 182 °C upwards the

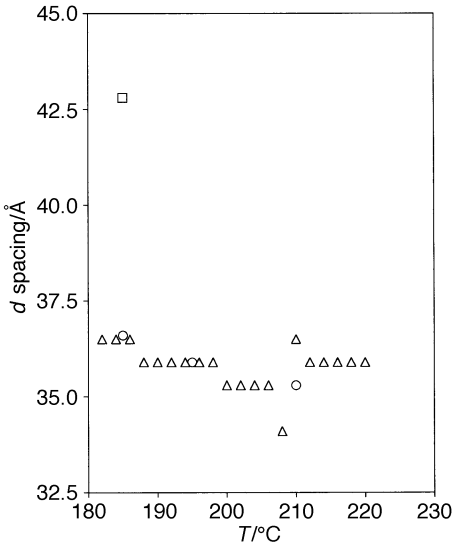

Fig. 8 Variation of the *d* spacings (layer thickness) of *N*-(4-decyloxybenzoyl)-*β*-D-glucopyranosylamine **9** with temperature; (□) reflections obtained for the crystalline phase *via* temperature scans at 2 °C min^{-1}, (○) reflections for the biphasic region, and (△) reflections for the liquid crystalline state, observed after heating from ambient temperature

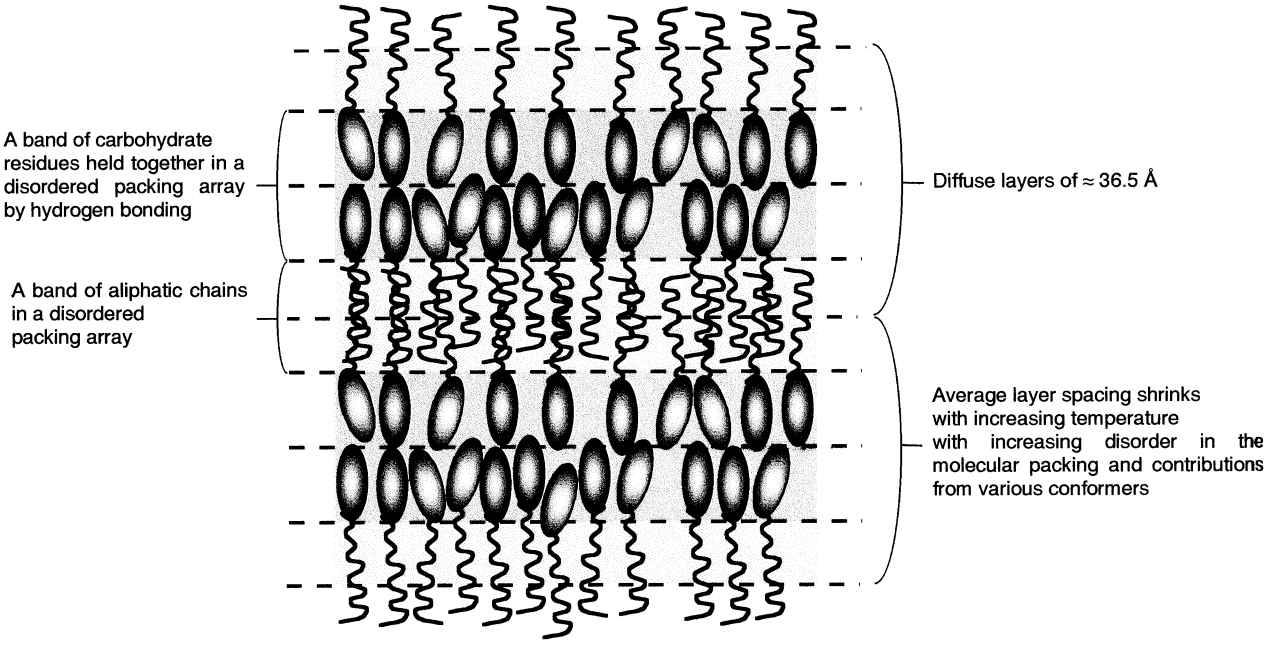

Fig. 6 A schematic model of the layer structure of *N*-octadecanoyl-*β*-D-glucopyranosylamine **28** in the smectic A* phase

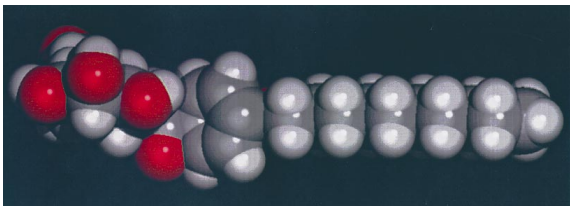

Fig. 7 A model of *N*-(4-decyloxybenzoyl)-*β*-D-glucopyranosylamine **9** obtained from CERIUS 2.0

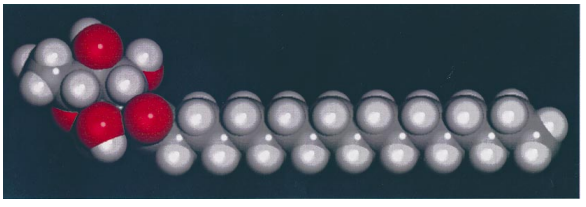

Fig. 9 A model of *N*-octadecanoyl-2-amino-2-deoxy-*β*-D-glucopyranose **29** obtained from CERIUS 2.0

Table 1 Melting points (°C) of the *N*-*trans*-(4-pentylcyclohexylcarbonyl)-*β*-D-glycopyranosylamines **1**–**3**

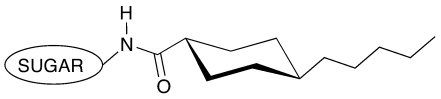

compound	sugar	Cr		I
1	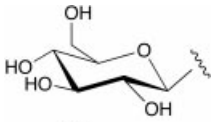	•	260 (decomp.)	•
2	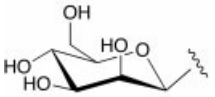	•	≈230 (decomp.)	•
3	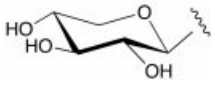	•	≈230 (decomp.)	•

Table 2 Transition temperatures (°C) for the *N*-(4-alkoxybenzoyl)-*β*-D-glucopyranosylamines **4**–**9**

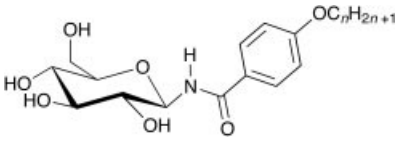

compound	*n*	Cr		SmA*		I
4	5	•	198		—	•
5	6	•	194	•	(178)[a]	•
6	7	•	187	•	199	•
7	8	•	191	•	214	•
8	9	•	181	•	220	•
9	10	•	187	•	224	•

[a]Represents a monotropic transition temperature.

Table 3 Melting points (°C) of the *N*-[4-*trans*-4-pentylcyclohexyl)-benzoyl]-*β*-D-glycopyranosylamines **10**–**13**

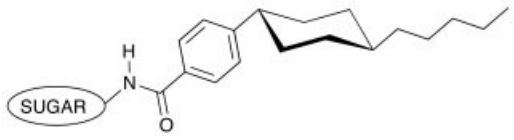

compound	sugar	Cr		I
10	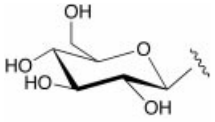	•	≈230 (decomp.)	•
11	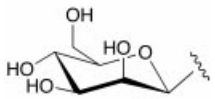	•	≈235 (decomp.)	•
12	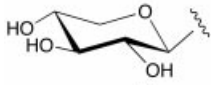	•	≈230 (decomp.)	•
13	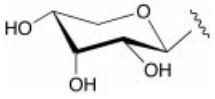	•	≈240 (decomp.)	•

Table 4 Melting points (°C) of variously substituted *N*-[4′-alkoxybiphenyl-4-ylcarbonyl)-*β*-D-mannopyranosylamines **14**–**17**

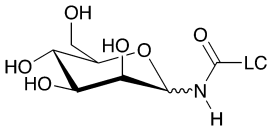

compound	LC	Cr		I
14	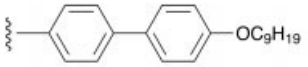	•	≈235 (decomp.)	•
15	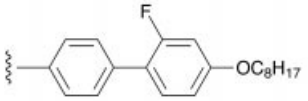	•	≈240 (decomp.)	•
16	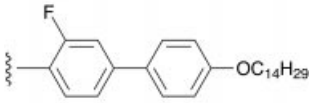	•	≈230 (decomp.)	•
17	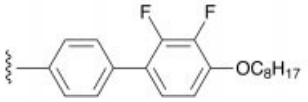	•	≈235 (decomp.)	•

Table 5 Transition temperatures (°C) for the 1-deoxy-1-(4-decyloxyphenyl)-*β*-D-glucopyranose **18**, 4-decyloxybenzyl-*β*-D-glucopyranose **19** and *N*-(4-decyloxybenzoyl)-*β*-D-glucopyranosylamine **9**

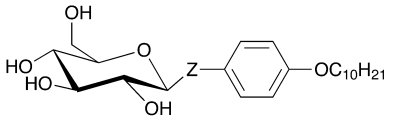

compound	Z	Cr		SmA*		I	ref.
18	—	•	107	•	173	•	41
19	OCH_2	•	117	•	166	•	44
9	NCHO	•	187	•	224	•	

absence of a maximum relating to d_1 and a fluctuation of the spacings d_2 between 36.5 and 34.1 Å, see Fig. 8. These values suggest the occurrence of an non-intercalated structure in the crystalline phase as opposed to an intercalated structure in the liquid-crystalline state as observed for *N*-octadecanoyl-*β*-D-glucopyranosylamine **28**. The small reduction of d_2 for **28** in the *d* spacing in the liquid-crystalline state and the reduction and then subsequent increase and broadening of the *d* spacing observed for **9**, which is unlike the behaviour generally observed in thermotropic liquid crystals, requires some consideration. Although any explanation of the behaviour of these partially oriented liquid-crystalline materials close to their isotropisation temperature has to be tentative, the concept of the nature of the liquid-crystalline state in carbohydrates offers some insight.[58] With rising temperatures the increased molecular motion and disordering can either be accommodated by a decreasing overlap of the alkyl chains, leading to increased *d* spacings, a feature not observed in the investigated materials, or by an increasing overlap of the carbohydrate groups leading to a decrease in the *d* spacing, but also to an expansion of the layers in their planes, required to allow for the overlap of the bulky head groups, and accommodating for the increased mobility of the flexible alkyl chains.

The reduced values of the intensities of the diffraction data and the broadening of the reflections for temperatures immediately preceding the isotropisation temperature suggest the onset of the breakdown of liquid-crystalline (long-range) order. The data correspond to the formation of species with periodicities between 27.6–45.5 Å. These lengths correspond roughly to

Table 6 Transition temperatures (°C) of the *N*-*trans*-4-pentylcyclohexylcarbonyl-*β*-D-glucopyranosylamine **1**, octyl *β*-D-glucopyranoside **20**, *trans*-4-butylcyclohexyl *β*-D-glucopyranoside **21**, 1-*O*-(*trans*-4-propylcyclohexyl)methyl *β*-D-glucopyranoside **22** and *N*-*trans*-4-pentylcyclohexylacetyl-*β*-D-glucopyranosylamine **23**

compound	structure	Cr		SmA*		I	ref.
20	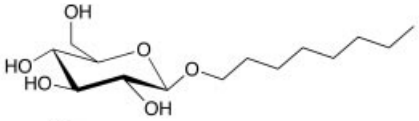	•	69	•	110	•	11
21	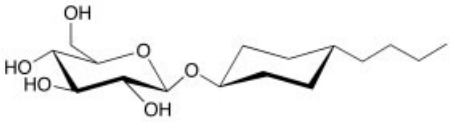	•	137	•	167	•	42
22	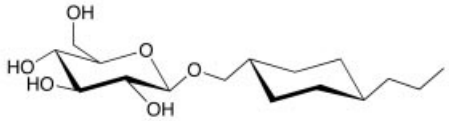	•	125	•	147	•	42
1	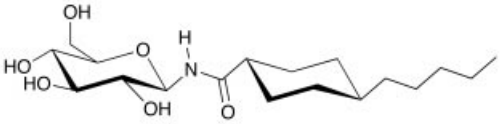	•	259	•	—	•	
23	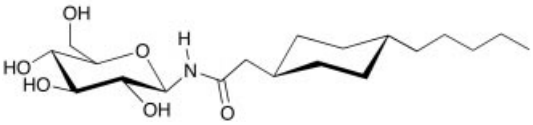	•	232	•	235	•	

the length of a single molecule and of a dimer. At higher temperatures thermal degradation sets in.

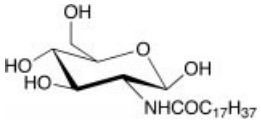

N-octadecanoyl-2-amino-2-deoxy-β-D-glucopyranose **29**; Cr–I, 197 °C[45,46]

As expected for *N*-octadecanoyl-2-amino-2-deoxy-*β*-D-glucopyranose **29**[45,46] liquid-crystalline behaviour was not observed. This is consistent with observations by optical microscopy and DSC.[45,46] However, between 182–194 °C intensities corresponding to values of 47.7–48.8 Å were detected, which compared to the maximum length of 28.1 Å of the compound, as determined by modelling and shown in Fig. 9, is indicative of a solid state of similar nature as observed for the other two materials.

Discussion

The *N*-(*trans*-4-pentylcyclohexylcarbonyl)-*β*-D-glycopyranosylamines **1**–**3** shown in Table 1 are not mesomorphic. The values recorded in the table are melting points (T_m) or the temperature at which significant visible decomposition occurs. The configuration of the carbohydrate moiety seems to be much less important than the high degree of hydrogen bonding attributable to the hydroxy groups on the carboyhydrate part of the molecule and the amino and carbonyl groups of the amide linkage in generating these high T_m values.

The transition temperatures and enthalpies of transition for the *N*-(4-alkoxybenzoyl)-*β*-D-glucopyranosylamines **4**–**9** are collated in Table 2. As usual liquid crystalline behaviour is found after a certain critical chain length ($n=6$) is reached. $T_{SmA^*\text{-}I}$ increases as the number of methylene units in the alkoxy chain increases. T_m is almost independent of chain length, as is often the case for liquid crystalline carbohydrates, although a general tendency of T_m to decrease with increasing chain length is apparent.

The replacement of the alkoxy chain in the *N*-(4-alkoxybenzoyl)-*β*-D-glucopyranosylamines **4**–**9** by a cyclohexyl ring to yield the *N*-[4-(*trans*-4-pentylcyclohexyl)benzoyl]-*β*-D-glucopyranosylamine **10**, shown in Table 3, suppresses the liquid crystalline behaviour by increasing T_m. No mesomorphism can be observed before decomposition occurs. This is also the case for the carbohydrates **10**–**12** where the incorporation of the additional 1,4-disubstituted phenylene ring into the esters **1**–**3** to yield the compounds **10**–**12** probably increases T_m, so that only decomposition is observed at elevated temperatures. The compound **13** is also non-mesomorphic below the decomposition temperature.

Increasing the size of the hydrophobic part in the liquid crystalline carbohydrate in the mannosylamine **2** and **11** with one phenyl ring to yield the mannosylamines **14**–**17** with two substituted phenyl rings again does not increase the tendency for liquid crystal formation, see Table 4. This implies that the incorporation of more than one aliphatic or aromatic ring into a liquid crystalline carbohydrate gives rise to such a high value for T_m that no liquid crystalline behaviour can be observed before decomposition takes place. This suggests that a normal alkyl chain or one alicyclic or aromatic ring is sufficient for mesophase formation at elevated temperatures. Attempts to actually lower T_m and $T_{SmA^*\text{-}I}$ would be more rewarding for practical applications, since solubility in water should increase.

The thermal data collated in Table 5 show that the presence of an additional site for hydrogen bonding in the linkage Z, *e.g.* an amide linkage in **9**, has a much greater influence on T_m and $T_{SmA^*\text{-}I}$ than the presence or absence of a linkage, *e.g.* compare $T_{SmA^*\text{-}I}$ for the compounds **18** and **19**.

The transition temperatures for the carbohydrates listed in Table 6 indicate that alicyclic rings, such as cyclohexane, lead to higher T_m and $T_{SmA^*\text{-}I}$; for example compare the thermal data for the compounds **20** and **21**. However, the data also imply that the odd numbers of units in the central linkage give rise to higher $T_{SmA^*\text{-}I}$ than an even number of units; see the data for compounds **20** and **21** and the compounds **1** and **23**.

Table 7 Transition temperatures (°C) of the 4-cyanophenyl *trans*-4-octylcyclohexanoate **24**, 4-cyanophenyl *trans*-4-(*trans*-4-pentylcyclohexyl)-cyclohexanecarboxylate **25**, 4-cyanophenyl *trans*-4-(*trans*-4-pentylcyclohexylmethyl)cyclohexanecarboxylate **26** and the 4-cyanophenyl *trans*-4-cyanophenyl *trans*-4-[2-(*trans*-4-pentylcyclohexyl)ethyl]cyclohexanecarboxylate **27**

compound	structure	Cr		SmB		N		I	ref.
24		•	62		—	•	79	•	59
25		•	92		—	•	232	•	60
26		•	110		—	•	(108)[a]	•	61
27	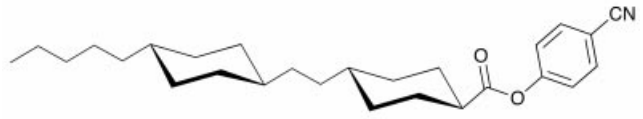	•	90	•	(65)[a]	•	197	•	61

[a]Represents a monotropic temperature.

An additional site of hydrogen bonding has a bigger influence on the transition temperatures than the nature of the linkage, compare **22** and **1**. This is exactly the opposite situation to that observed for the thermotropic liquid-crystalline behaviour of non-amphiphilic liquid crystals. This is illustrated clearly by the thermal data collated in Table 7 for a number of non-amphiphilic liquid crystals incorporating cyclohexane rings (**24**–**27**). It is evident that the compounds with an aliphatic ring incorporating no linkage (**25**) or an even number of carbon atoms (**27**) exhibit significantly higher clearing points than that (**26**) with an odd number of carbon atoms in the linkage. This has been attributed to the linear conformation of the former and a bent or kinked conformation for the latter.

Conclusions

The amide linkage in liquid crystalline carbohydrates generally gives rise to high transition temperatures and to insolubility, at least in the pyranose form, in water. This is probably due to a high degree of intermolecular hydrogen bonding also involving the amide linkage. There is no correlation between the thermotropic liquid crystalline behaviour of non-amphiphilic and amphiphilic liquid crystals as a function of molecular structure. This is exemplified by the opposite odd-even effect on the mesomorphic behaviour of the central linkage between the hydrophilic and hydrophobic parts of liquid crystalline carbohydrates and that of related non-amphiphilic liquid crystals. The presence of alicyclic rings, such as cyclohexane, or more than one phenyl ring, or combinations of cyclohexane and phenyl rings leads to such high melting points that no mesomorphism can be observed before thermal decomposition occurs. A non-intercalated structure is found for the crystalline state of the carbohydrates investigated. The chains appear to adopt an intercalated structure in the smectic A* phase after melting has occurred.

We gratefully acknowledge the EPSRC for support of post-graduate (M. G.), postdoctoral (P. L. and G. M.) and Advanced Fellowships (S. M. K.). Mrs B. Worthington (^{1}H NMR), Mr R. Knight (IR), C. Kennedy (CHN) and Mr A. D. Roberts (MS) are thanked for their assistance.

References

1 M. Berthelot, *Compt. Rend.*, 1855, **41**, 452; *J. Prakt. Chem.*, 1856, **671**, 235.
2 E. Fischer and B. Helferich, *Liebigs Ann. Chem.*, 1911, **383**, 68.
3 A. H. Salway, *J. Chem. Soc.*, 1913, **103**, 1022.
4 P. Gaubert, *Compt. Rend.*, 1919, **168**, 277.
5 V. Vill, H. Kelkenberg and J. Thiem, *Liq. Cryst.*, 1992, **11**, 459.
6 C. R. Noller and W. C. Rockwell, *J. Am. Chem. Soc.*, 1938, **60**, 2076.
7 J. C. Chabala and T. Y. Shen, *Carbohydr. Res.*, 1978, **67**, 55.
8 E. Barral, B. Grant, M. Oxsen, E. T. Samulski, P. C. Moews, J. R. Knox, R. R. Gaskill and J. L. Haberfeld, *Org. Coat. Plast. Chem.*, 1979, **40**, 67.
9 V. Vill, *Mol. Cryst. Liq. Cryst.*, 1992, **213**, 67.
10 J. W. Goodby, *Mol. Cryst. Liq. Cryst.*, 1984, **110**, 205.
11 G. A. Jeffrey, *Acc. Chem. Res.*, 1986, **19**, 168.
12 G. A. Jeffrey and L. M. Wingert, *Liq. Cryst.*, 1992, **12**, 179.
13 G. A. Jeffrey and S. Bhattacharjee, *Carbohydr. Res.*, 1983, **115**, 53.
14 H. A. van Doren and L. M. Wingert, *Mol. Cryst. Liq. Cryst.*, 1991, **198**, 381.
15 R. G. Zimmermann, G. B. Jameson, R. Weiss and G. Demailly, *Mol. Cryst. Liq. Cryst., Lett.*, 1985, **1**, 183.
16 B. Kohne, W. Praefcke, W. Stephan and P. Nürnberg, *Z. Naturforsch., Teil B*, 1985, **40**, 981.
17 W. V. Dahlhoff, *Z. Naturforsch., Teil B*, 1987, **42**, 661.
18 B. Pfannemüller, W. Welte, E. Chin and J. W. Goodby, *Mol. Cryst. Liq. Cryst.*, 1986, **1**, 357.
19 M. Marcus and P. L. Finn, *Liq. Cryst.*, 1988, **30**, 381.
20 Y. J. Chung and G. A. Jeffrey, *Biochim. Biophys. Acta*, 1989, **985**, 300.
21 T. E. Thomson and A. Baron, *Biochim. Biophys. Acta*, 1975, **382**, 276.
22 J. Diesenhofer and H. Michel, *Angew. Chem.*, 1989, **101**, 872.
23 E. Lederer, *Chem. Phys. Lipids*, 1976, **16**, 91.
24 D. Asselineau and J. Asselineau, *Prog. Chem. Fats Other Lipids*, 1978, **16**, 59.
25 H. Arita, K. Sugita, A. Nomura, K. Sato and J. Kawanami, *Carbohydr. Res.*, 1978, **62**, 143.
26 K. Hill, in *Carbohydrates as Raw Materials II*, ed. G. Descotes, VCH Verlag, Weinheim, 1993, p. 163 and references therein.
27 J. G. Riess and J. Greiner, in *Carbohydrates as Raw Materials II*, ed. G. Descotes, VCH Verlag, Weinheim, 1993, p. 209 and references therein.
28 M. J. Lawrence, *Chem. Soc. Rev.*, 1994, 417.
29 V. Vill, H.-W. Tunger and M. Paul, *J. Mater. Chem.*, 1995, **6**, 2283.
30 V. Vill, H.-W. Tunger and M. von Minden, *J. Mater. Chem.*, 1996, **6**, 739.
31 *Structure of Biological Membranes*, ed. S. Abrahamson and I. Pascher, 1977, Plenum Press, New York.

32 *Liquid Crystals and Biological Systems*, ed. J. J. Wolken and G. H. Brown, 1980, Academic Press, New York.
33 J. W. Goodby, J. A. Haley, G. Mackenzie, M. J. Watson, D. Plusquellec and V. Ferrières, *J. Mater. Chem.*, 1995, **5**, 2209.
34 J. W. Goodby, J. A. Haley, G. Mackenzie, M. J. Watson, S. M. Kelly, P. Lettelier, O. Douillet, P. Godé, G. Goethals, G. Ronco and V. Villa, *Liq. Cryst.*, 1997, **22**, 367.
35 J. W. Goodby, J. A. Haley, G. Mackenzie, M. J. Watson, S. M. Kelly, P. Lettelier, O. Douillet, P. Godé, G. Goethals, G. Ronco, B. Harmouch, P. Martin and V. Villa, *Liq. Cryst.*, 1997, **22**, 497; *J. Carbohydr. Chem.*, 1997, **16**, 479.
36 P. Lettelier, D. F. Ewing, J. W. Goodby, J. A. Haley, S. M. Kelly and G. Mackenzie, *Liq. Cryst.*, 1997, **22**, 609.
37 H. Prade and R. Miethchen, *Carbohydr. Lett.*, 1994, **1**, 19.
38 H. Prade, R. Miethchen and V. Vill, *J. Prakt. Chem.*, 1995, **337**, 427.
39 P. Stangier, V. Vill, S. Rohde, U. Jeschke and J. Thiem, *Liq. Cryst.*, 1994, **17**, 589.
40 V. Vill, T. Böcker, J. Thiem and F. Fischer, *Liq. Cryst.*, 1989, **6**, 349.
41 G. A. Jeffrey, *Mol. Cryst. Liq. Cryst.*, 1984, **110**, 221.
42 C. Tschierske, A. Lunow and H. Zaschke, *Liq. Cryst.*, 1990, **8**, 885.
43 D. Joachimi, C. Tschierschke, H. Müller, J. H. Wendorff, L. Schneider and R. Kleppinger, *Angew. Chem., Int. Ed. Engl.*, 1993, **32**, 1165.
44 P. Lettelier, D. F. Ewing, J. W. Goodby, J. A. Haley, S. M. Kelly and G. Mackenzie, *Liq. Cryst.*, 1997, **22**, 609.
45 D. F. Ewing, M. Glew, J. W. Goodby, J. A. Haley, S. M. Kelly, P. Lettelier and G. Mackenzie, Proceedings of the 26th Freiburger Arbeitstagung Flüssigkristalle, Freiburg, Germany, 1997, p. 55.
46 D. F. Ewing, J. W. Goodby, J. A. Haley, S. M. Kelly, P. Lettelier and G. Mackenzie, *Liq. Cryst.*, 1997, **23**, 759.
47 P. Leon-Ruaud, M. Allainmat and D. Plusquellec, *Tetrahedron Lett.*, 1991, 1557.
48 H. Kunz, *Angew. Chem., Int. Ed. Engl.*, 1987, **26**, 294.
49 U. Jeschke, C. Vogel, V. Vill and H. Fischer, *J. Mater. Chem.*, 1995, **5**, 2073.
50 H. A. van Doren, R. van der Geest, C. F. de Ruijer, R. M. Kellogg and H. Wynberg, *Liq. Cryst.*, 1990, **8**, 109.
51 B. Pfannemüller and W. Welte, *Chem. Phys. Lipids*, 1985, **37**, 227.
52 D. Baeyens-Volant, P. Cuvelier, R. Fornasier, E. Szalai and C. David, *Mol. Cryst. Liq. Cryst.*, 1985, **128**, 277.
53 D. Baeyens-Volant, R. Fornasier, E. Szalai and C. David, *Mol. Cryst. Liq. Cryst.*, 1986, **135**, 93.
54 J. A. Boustra, G. S. Gooris, W. Bras and H. Talsma, *Chem. Phys. Lipids*, 1993, **64**, 83.
55 W. Bras and J. A. Boustra, *NIMPR*, 1993, A326, 587.
56 E. Towns-Andrews, A. Berry, J. G. Bordas, R. Mant, P. K. Murray, K. Roberts, I. Summer, J. S. Worgan, R. Lewis and A. Gabriel, *Rev. Sci. Instrum.*, 1989, **60**, 2346.
57 W. Folkhard, W. Geercken, E. Knoerzler, E. Mosler, H. Nemetschek-Gansler, T. Nemetschek and M. H. J. Koch, *J. Mol. Biol.*, 1987, **193**, 405.
58 I. Pascher and S. Sundell, *Chem. Phys. Lipids*, 1977, **20**, 171.
59 H.-J. Deutscher, F. Kuschel, S. König, H. Kresse, D. Pfeiffer, A. Wiegeleben, J. Wulf and D. Demus, *Z. Chem. (Leipzig)*, 1977, **17**, 64.
60 R. Eidenschink, *Kontakte*, 1977, **1**, 15.
61 H.-J. Deutscher, R. Frach and R. Krieg, 1986, Proceedings of the 16th Freiburger Arbeitstagung Flüssigkristalle, Freiburg, Germany.

Paper 7/07013F; *Received* 29*th September*, 1997